

Detection and Mechanistic Studies of Multicomponent Assembly by Fluorescence Resonance Energy Transfer

Ronald K. Castellano,^{†,‡} Stephen L. Craig,[†] Colin Nuckolls,[†] and Julius Rebek, Jr.^{*,†}

Contribution from the The Skaggs Institute for Chemical Biology and the Department of Chemistry, The Scripps Research Institute, La Jolla, California 92037, and the Department of Chemistry, Massachusetts Institute of Technology, Cambridge, Massachusetts 02139

Received December 16, 1999

Abstract: The kinetics and thermodynamics of multicomponent assembly in organic solution are investigated using fluorescence resonance energy transfer (FRET). Calix[4]arenes functionalized with ureas on their wider rims dimerize in organic solution, via intermolecular hydrogen bonding, to form encapsulation complexes. When one calixarene component is outfitted with a donor fluorophore and the other with an acceptor, dimerization brings the chromophores within 20 Å, a distance suitable for efficient energy transfer to occur between them. Excitation of the donor results in two colors of emitted light: one fluorescence band at the donor emission wavelength, and a second at the acceptor emission wavelength signaling the noncovalent union of three species—donor, acceptor, and small-molecule guest. By monitoring these wavelengths, assembly and dissociation processes are observed in real time at nanomolar concentrations. Rate and association constants for assembly processes are determined for the first time, and they reveal unexpected contributions from the structure and concentration of the monomer. Finally, the combination of FRET and the molecular recognition capabilities of the encapsulation complexes provides a sensitive and specific method for small-molecule sensing.

Introduction

Calixarenes functionalized with ureas on their wider rims form discrete dimers in organic solution (Figure 1).^{1,2} These capsular structures are held together by a seam of 16 hydrogen bonds, and their interiors are large enough to accommodate molecular guests. The assemblies are capable of a variety of chemical tasks. For example, the presence of a suitable guest is a necessary condition for assembly and the host capsule is selective toward the size, shape, and chemical functionality of the encapsulated guest.¹ The direction of the hydrogen bond seam imparts chirality into capsules formed from nonidentical monomers, and chirality can be transferred from substituents on the ureas to the capsule interior.³ The dimer is also the basis of a platform for reversible polymeric materials that exhibit a wide range of structural, physical, and dynamic properties.⁴

The dynamics and thermodynamics of dimerization are central to the function of the assemblies, but little quantitative informa-

tion has been determined. The encapsulation complexes have been studied by NMR,^{1–4} circular dichroism (CD) spectroscopy,^{3b} electrospray mass spectrometry,⁵ and X-ray crystallography,^{2b} and of those only NMR and CD offer a glimpse of the reversible solution dynamics of the assemblies. Even so, there is a limited knowledge of the rates and equilibria of dimerization because at millimolar concentrations the assembly process is too rapid^{4d} and too complete⁶ to be fully quantified; only dissociation rates have been measured.^{2c,e}

We report here the use of fluorescence resonance energy transfer (FRET) to investigate multicomponent, hydrogen-bonded assemblies in organic solution. FRET⁷ is widely used to study dynamic processes in biological systems, including conformational changes⁸ and self-assembly,⁹ at low concentrations and on rapid time scales. The sensitivity of the technique

[†] The Scripps Research Institute.

[‡] Massachusetts Institute of Technology.

* To whom correspondence should be addressed.

(1) (a) Shimizu, K. D.; Rebek, J., Jr. *Proc. Natl. Acad. Sci. U.S.A.* **1995**, *92*, 12403–12407. (b) Hamann, B. C.; Shimizu, K. D.; Rebek, J., Jr. *Angew. Chem., Int. Ed. Engl.* **1996**, *35*, 1326–1329. (c) Castellano, R. K.; Rudkevich, D. M.; Rebek, J., Jr. *J. Am. Chem. Soc.* **1996**, *118*, 10002–10003.

(2) (a) Mogck, O.; Böhmer, V.; Vogt, W. *Tetrahedron* **1996**, *52*, 8489–8496. (b) Mogck, O.; Paulus, E. F.; Böhmer, V.; Thondorf, I.; Vogt, W. *Chem. Commun.* **1996**, 2533–2534. (c) Mogck, O.; Pons, M.; Böhmer, V.; Vogt, W. *J. Am. Chem. Soc.* **1997**, *119*, 5706–5712. (d) Böhmer, V.; Mogck, O.; Pons, M.; Paulus, E. F. Reversible Dimerization of Tetraarenes Derived From Calix[4]arenes. In *NMR in Supramolecular Chemistry*; M. Pons, ed.; NATO ASI Ser., Ser. C, Vol. 526; Kluwer Academic Publishers: Dordrecht, The Netherlands, **1999**; pp 45–60. (e) Vysotsky, M. O.; Thondorf, I.; Böhmer, V. *Angew. Chem., Int. Ed. Engl.* **2000**, *39*, 1264–1267.

(3) (a) Castellano, R. K.; Kim, B. H.; Rebek, J., Jr. *J. Am. Chem. Soc.* **1997**, *119*, 12671–12672. (b) Castellano, R. K.; Nuckolls, C.; Rebek, J., Jr. *J. Am. Chem. Soc.* **1999**, *121*, 11156–11163.

(4) (a) Castellano, R. K.; Rudkevich, D. M.; Rebek, J., Jr. *Proc. Natl. Acad. Sci. U.S.A.* **1997**, *94*, 7132–7137. (b) Castellano, R. K.; Rebek, J., Jr. *J. Am. Chem. Soc.* **1998**, *120*, 3657–3663. (c) Castellano, R. K.; Nuckolls, C.; Eichhorn, S. H.; Wood, M. R.; Lovinger, A. J.; Rebek, J., Jr. *Angew. Chem., Int. Ed. Engl.* **1999**, *38*, 2603–2606. (d) Castellano, R. K.; Nuckolls, C.; Rebek, J., Jr. *Polym. News* **2000**, *25*, 44–52. (e) Nuckolls, C.; Castellano, R. K.; Rebek, J., Jr. *Polym. Prepr.* **2000**, *41*, 930–931. (f) Castellano, R. K.; Clark, R.; Craig, S. L.; Nuckolls, C.; Rebek, J., Jr., submitted for publication.

(5) Schalley, C. A.; Castellano, R. K.; Brody, M. S.; Rudkevich, D. M.; Siuzdak, G.; Rebek, J., Jr. *J. Am. Chem. Soc.* **1999**, *121*, 4568–4579.

(6) Calixarenes featuring aryl ureas have been shown to be exclusively dimeric at the dilution limit of the 600 MHz NMR spectrometer—72 μ M in CDCl₃ (295K): Castellano, R. K.; Rebek, J., Jr., unpublished work.

(7) For reviews on FRET theory and applications, see: (a) Wu, P.; Brand, L. *Anal. Biochem.* **1994**, *218*, 1–13. (b) Clegg, R. M. *Curr. Opin. Biotechnol.* **1995**, *6*, 103–110. (c) Selvin, P. R. *Methods Enzymol.* **1995**, *246*, 300–334. (d) Yang, M.; Millar, D. P. *Methods Enzymol.* **1997**, *278*, 417–444. (e) Szöllösi, J.; Damjanovich, S.; Mátyus, L. *Cytometry* **1998**, *34*, 159–179. (f) Tsien, R. Y.; Miyawaki, A. *Science* **1998**, *280*, 1954–1955.

(8) For a recent example, see: Ha, T.; Zhuang, X.; Kim, H. D.; Orr, J. W.; Williamson, J. R.; Chu, S. *Proc. Natl. Acad. Sci. U.S.A.* **1999**, *96*, 9077–9082 and references therein.

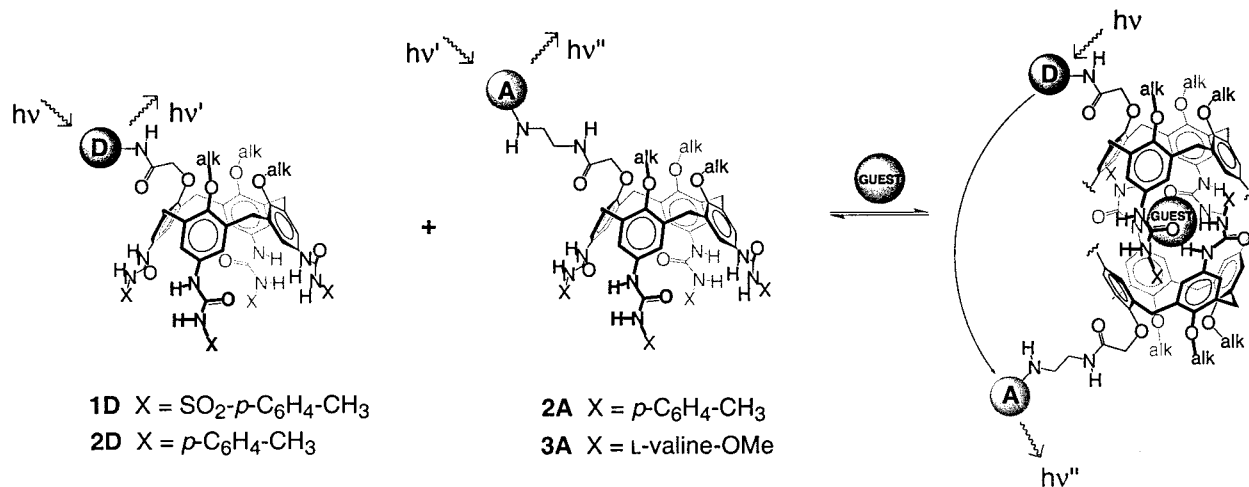


Figure 1. A donor chromophore (D) and an acceptor chromophore (A), in the presence of a guest, are brought within FRET distance upon the dimeric assembly of calix[4]arene tetraureas. Some groups have been omitted for clarity. (alk = C₁₀H₂₁).

allows detection of interacting species at nanomolar concentrations. At these low concentrations, the individual (“free”) components as well as the assemblies can be observed directly, assembly/dissociation processes can be observed in real time, and equilibria can be determined that are not accessible at the millimolar concentrations that are required for NMR analysis.

The experimental design is described in Figure 1. Calixarene monomers are tagged with donor (D) and acceptor (A) fluorophores, and dimerization (A•D) brings them within 20 Å of one another.¹⁰ The fluorophores are chosen so that the emission spectrum of D overlaps the absorption spectrum of A, and nonradiative energy transfer occurs between them upon irradiation (*hν*).¹¹ Because A is also a fluorophore, the energy transfer process can be monitored at both the emission maximum of D (*hν'*) and that of A (*hν''*). Energy transfer is extremely efficient, so that a fluorescence signal at *hν''* indicates the noncovalent union of three species—donor, acceptor, and guest.

We report here the kinetics and thermodynamics of calixarene dimerization for several capsules in different solvents. The mechanistic studies provide insight into the structure and thermodynamics of monomers as well as the dimeric assemblies. These experiments greatly expand the concentration range at which assembly can be observed, and we find that calixarene concentration has an unexpected effect on the dissociation rates of the dimers. Finally, we show that the combination of fluorescence and the molecular recognition properties of the dimers holds promise for specific small-molecule sensing.

Results and Discussion

Preparation of Dye-Labeled Calixarenes. For these studies, modified coumarin laser dyes—coumarin 2 as the donor and coumarin 343 as the acceptor (Figure 2)—were connected to the appropriate calixarene platforms via amide linkages using the synthetic procedures outlined in Schemes 1 and 2. This FRET pair has recently been employed by Fréchet and co-

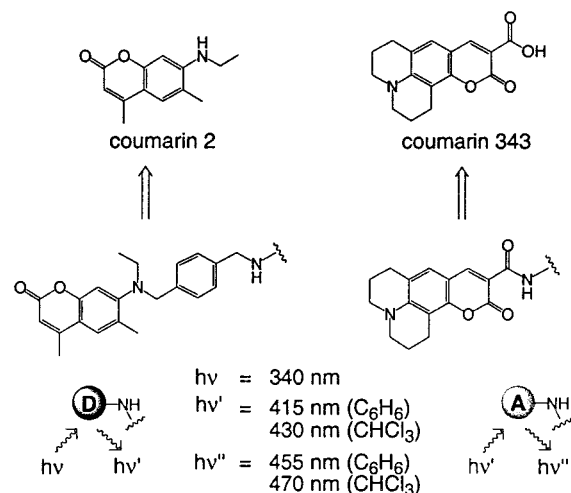


Figure 2. The donor (coumarin 2) and the acceptor (coumarin 343) dyes can be easily modified for connection to the calixarene scaffold.

workers in their light-harvesting dendrimers.¹² Donor-tagged tetrasulfonyl urea **1D** and tetraaryl urea **2D** were prepared in one step through the PyBOP-mediated coupling of modified coumarin 343, **6**, to the appropriate monoacid precursor, either **4** or **5** (Scheme 1). Through similar strategies, the aryl urea ethylene amine derivative **8** was prepared and coupled directly to the acid function of coumarin 2 (Scheme 2) to afford **2A**.

Control Experiments. The fluorescence spectra of simple *tert*-butyl control compounds **9D** and **9A** (Figure 3) confirm that their absorption and emission maxima in chloroform and benzene are essentially identical to the parent coumarin chromophores^{12c} and the tetraurea derivatives (Figure 2)—the amide connectivity does not significantly change the electronic properties of the dyes.¹³ Dilution studies performed with equimolar mixtures of **9D** and **9A** establish the concentration range wherein energy transfer no longer occurs between the *free* dyes in solution (Figure 4a). Considerable FRET is observed at 5 μM in chloroform, evidenced by the pronounced acceptor

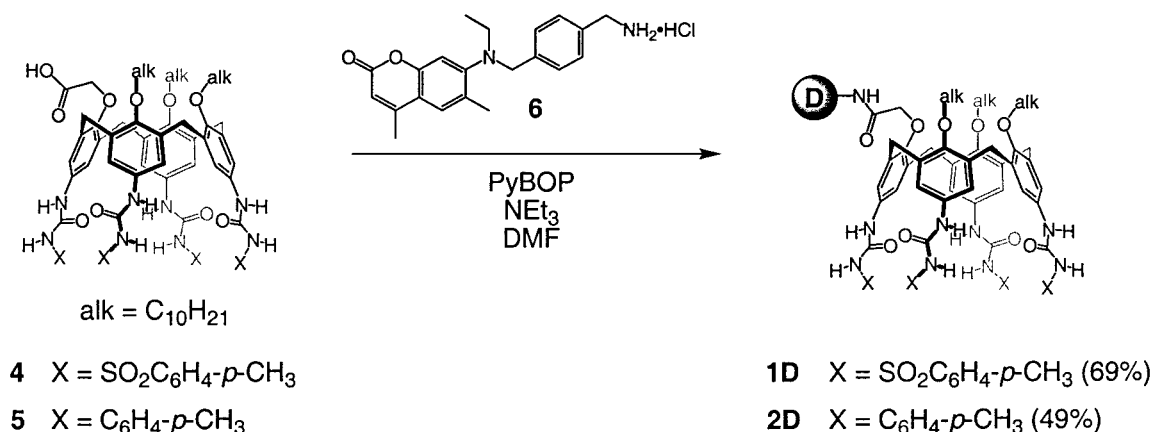
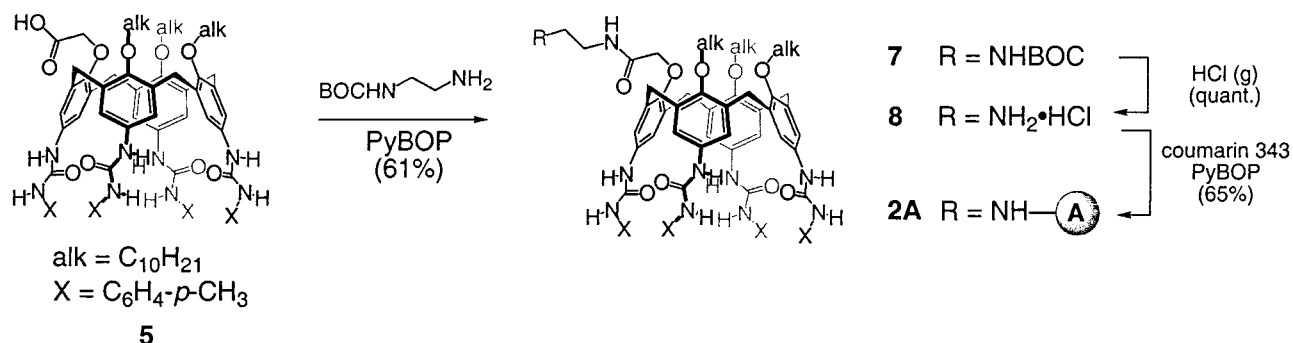
(9) For a recent example, see: Gelfand, C. A.; Plum, G. E.; Mielewicz, S.; Remeta, D. P.; Breslauer, K. J. *Proc. Natl. Acad. Sci. U.S.A.* **1999**, *96*, 6113–6118.

(10) Within the presumed Förster distance of the FRET dye pair (typically <80 Å). See ref 7a.

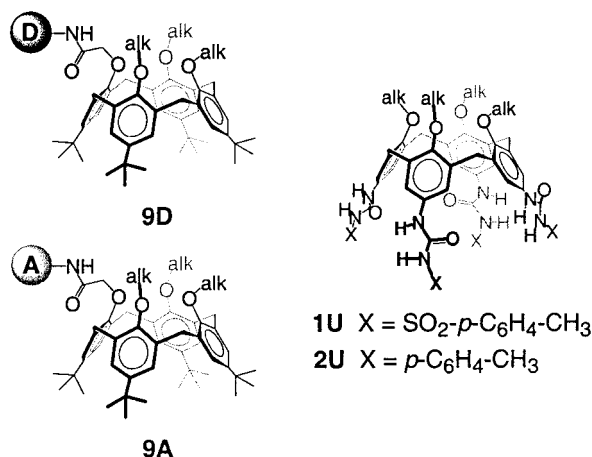
(11) For energy transfer in other neutral, hydrogen-bonded assemblies, see: (a) Ward, M. D. *Chem. Soc. Rev.* **1997**, *26*, 365–375 and references therein. (b) Springs, S. L.; Gosztola, D.; Wasielewski, M. R.; Král, V.; Andrievsky, A.; Sessler, J. L. *J. Am. Chem. Soc.* **1999**, *121*, 2281–2289 and references therein.

(12) (a) Gilat, S. L.; Adronov, A.; Fréchet, J. M. J. *Angew. Chem., Int. Ed. Engl.* **1999**, *38*, 1422–1427. (b) Gilat, S. L.; Adronov, A.; Fréchet, J. M. J. *J. Org. Chem.* **1999**, *64*, 7474–7484. (c) Adronov, A.; Gilat, S. L.; Fréchet, J. M. J.; Ohta, K.; Neuwahl, F. V. R.; Fleming, G. R. *J. Am. Chem. Soc.* **2000**, *122*, 1175–1185.

(13) N-alkylation of coumarin 2 does cause a decrease in molar absorptivity. See ref 12c for details.

Scheme 1. Synthesis of the Donor-Tagged Tetraureas **1D** and **2D** (alk = C₁₀H₂₁)**Scheme 2.** Synthesis of the Acceptor-Tagged Aryl Urea **2A** (alk = C₁₀H₂₁)

emission signal at 465 nm. This band essentially disappears upon 10-fold dilution and only a small shoulder remains—irradiation of the donor at these concentrations gives only donor emission.¹⁴ In related experiments, the donor control **9D** is combined with the aryl urea acceptor **2A**, 1:1 in chloroform (Figure 4b). At the three highest concentrations investigated, **2A** is dimeric, and likely not aggregating with the *tert*-butyl donor. The results of the experiment again suggest that the two coumarin dyes form an extremely efficient FRET pair. These dilution experiments have important consequences for the assembly of donor- and acceptor-labeled calixarene tetraureas—an appreciable FRET signal arising from their combination at concentrations below ~500 nM must indicate an aggregation event (“intra-assembly” FRET). Moreover, at higher concentrations some contribution from “inter-assembly” FRET can be expected.

**Figure 3.** Various tagged and untagged calixarenes used in the control experiments. (alk = C₁₀H₂₁).

“Intra-Assembly” Energy Transfer. Calixarenes **1D** and **2A**, featuring sulfonyl ureas and aryl ureas, respectively, have been shown to form exclusively heterodimeric pairs in solution,^{3a,4b} so that the combination of these two species was expected to give a large excess of the desired FRET complex. Figure 5a shows the change in the emission spectrum with time upon mixing 100 nM each of **1D** and **2A** in chloroform. Initially, the donor and acceptor are isolated from each other in solution, and only emission from the donor is observed. Over the course of hours, the heterodimer **1D**•**2A** forms, energy transfer occurs, and the acceptor emission increases until essentially quantitative energy transfer is observed. That the FRET signal depends on assembly is evident from (a) the slow onset; energy transfer between free monomers would be observed immediately, (b) the concentration; energy transfer between the “free” dyes is precluded based on the control dilution experiments, and (c) the insensitivity of the emission intensity to added (excess) acceptor.

Finally, by titrating the dimer solution with a solvent that can effectively compete for the hydrogen bonds, such as dimethyl sulfoxide (DMSO), this process can be reversed, restoring the donor emission (Figure 5b).¹⁵ Unlike the association processes, which take minutes to hours to reach equilibrium, “denaturation” is complete within seconds of adding DMSO. The spectra pass through the same isosbestic point in both the assembly and dissociation sequences, underscoring the reversibility of the process.¹⁶

(14) Throughout all of these experiments ca. 10% of the acceptor emission signal arises from its direct excitation.

(15) Control experiments determined the inherent sensitivities of the dyes to DMSO. The emission intensity of *both* the donor and acceptor controls gradually increased upon titration (at 1% DMSO, 14% increase for the donor, 10% increase for the acceptor). See the Supporting Information for details.

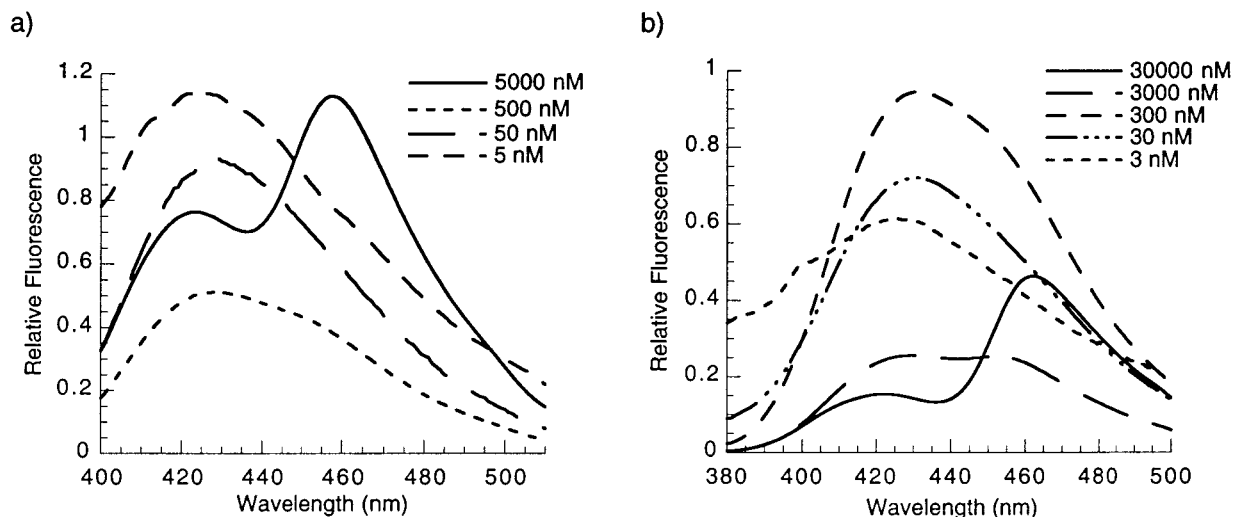


Figure 4. Dilution experiments in chloroform establish the concentration threshold for FRET between the “free” dyes in solution: (a) with 1:1 mixtures of **9D** and **9A**; (b) with 1:1 mixtures of **9D** and **2A**.

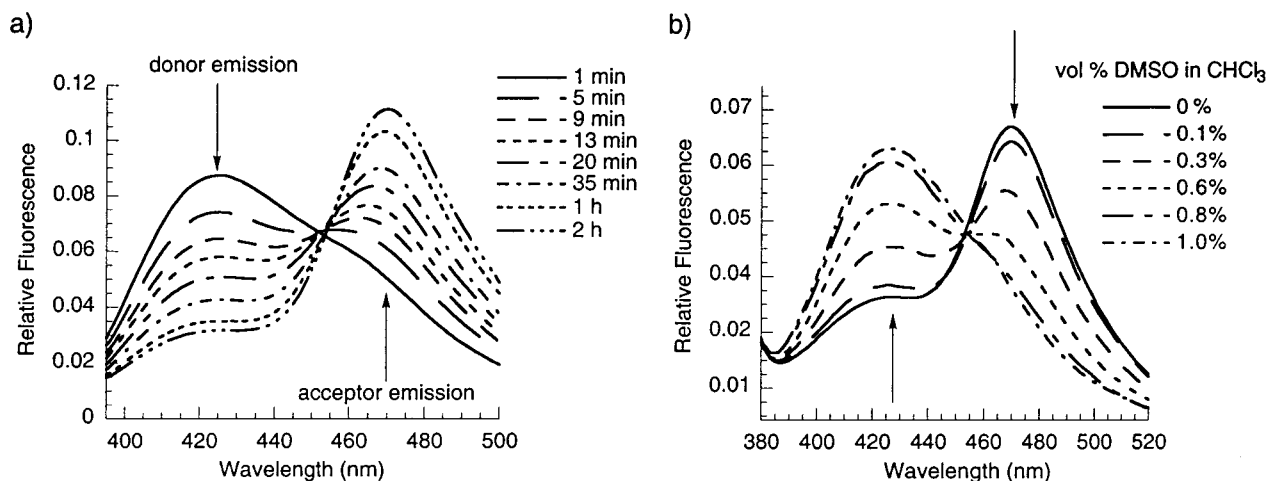


Figure 5. (a) FRET occurs upon combination of **1D** and **2A** at 100 nM in chloroform and the emission of the acceptor grows in as **1D·2A** forms—a process that takes hours. (b) Added DMSO instantaneously reverses the assembly of **1D·2A** in CHCl_3 , as indicated by restoration of the donor emission signal.

Rate and Equilibrium Constants. The association rate constant for assembly of **1D** and **2A**, k_{ass} , was measured by using an excess of **1D** and simultaneously monitoring the donor and acceptor emission intensities (Figure 6). The observed pseudo-first-order kinetics yield an apparent rate constant for dimer formation (Figure 6, inset). The apparent rate constant reflects not only the desired second-order rate constant, but also the concentrations of free monomers **2A** and **1D** in solution. Accurate association rate constants were obtained from studies at low concentrations (10 nM) of **2A** where essentially all of the calixarene exists as free monomer. Rate constants for association in both chloroform and benzene are reported in Table 1.

Dissociation rates were obtained from two similar experiments. The dissociation rate constant (k_{diss}) for **2·2**, for example, came from measuring either the appearance of the FRET signal upon mixing **2A·2A** and **2D·2D** or the disappearance of the FRET signal upon mixing **2A·2D** (in equilibrium with **2A·2A** and **2D·2D**) with untagged **2U·2U** (Figure 3). The dissociation constant of **1·2** was obtained from the disappearance of FRET upon mixing **1D·2A** with an excess of untagged **1U**. The

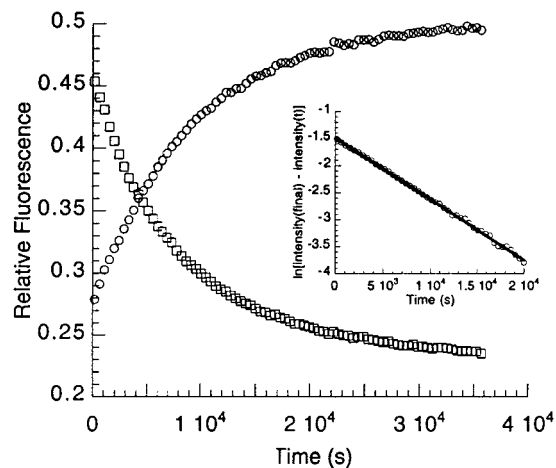


Figure 6. Change in fluorescence intensity with time of the donor emission maximum (415 nm, squares) and acceptor intensity maximum (455 nm, circles) upon combination of **2A** (100 nM) and **1D** (250 nM) in benzene at 25 °C. Inset: Pseudo-first-order kinetic treatment of the data.

association and dissociation rate constants for **1D·2A** were combined to give the equilibration association constant K_A for the assembly.

(16) For DMSO denaturation experiments monitored by FRET in a biological context, see: Garzon-Rodriguez, W.; Sepulveda-Becerra, M.; Milton, S.; Glabe, C. G. *J. Biol. Chem.* **1997**, *272*, 21037–21044.

Table 1. Rate and Association Constants for the Assembly and Dissociation of Calixarene Tetraureas in Chloroform and Benzene as Measured by FRET at Concentrations of 0.05–0.5 μM

	solvent	k_{ass} ($\text{M}^{-1} \text{s}^{-1}$) ^a	k_{diss} (s^{-1}) ^a	K_{A} (M^{-1}) ^a
1·1	CHCl_3	— ^b	— ^b	— ^b
1·2	CHCl_3	$2.7^b \times 10^3$	2.3×10^{-5}	1.2×10^8
2·2	CHCl_3	1.5×10^4	6.4×10^{-3}	2.4×10^6
1·1	C_6H_6	<50	5.4×10^{-5}	< 10^6
1·2	C_6H_6	3×10^3	5×10^{-6}	6×10^8
2·2	C_6H_6	2.4×10^4	6×10^{-4}	4×10^7

^a Uncertainties in k_{diss} are $\pm 15\%$, and in k_{ass} and K_{A} are $\pm 40\%$.

^b Compound **1** does not appear to form a well-defined dimer in CHCl_3 by NMR,³ and its behavior in this work is consistent with a species that is effectively monomeric at these concentrations.

The association constants of **2·2** were derived from the concentration dependencies of heterodimerization rates. It was assumed that the rate at which **1D** is converted to **1D·2A** is proportional to the concentration of free monomer **2A** in solution. When **1D** was mixed with **2A**, therefore, the apparent pseudo-first-order rate constant was divided by the value of k_{ass} from the low-concentration studies to give the concentration of free **2A**. The concentration of free **2A** and calculated concentration of dimeric **2A·2A** ([total **2A** – free **2A**]/2) were converted into an association constant. Experiments across a range of concentrations and stoichiometries were internally consistent and agreed with approximate association constants derived from the amount of FRET observed as a function of concentration of **2A·2D**. The combination of K_{A} and k_{diss} was used to calculate k_{ass} , and a range of experiments gave the assembly parameters in chloroform and benzene that are reported in Table 1.

The measured association constants (K_{A} values) are largely consistent with previous observations. The K_{A} for **2·2** in chloroform, $2.4 \times 10^6 \text{ M}^{-1}$, is higher than the lower limit set by NMR⁶ and in excellent agreement with recent quasi-elastic light scattering results.¹⁷ The K_{A} of **1·2** is $\sim 50\times$ greater than that of **2·2**, which agrees qualitatively with the preference for heterodimerization observed by NMR.^{3a,4b} In all cases, the K_{A} values are higher and dissociation rates are slower in benzene than in the more polar chloroform, and the kinetic and equilibrium measurements are self-consistent.

The dissociation constants, however, are much slower than expected. Our k_{diss} value for the aryl urea homodimer **2·2** in benzene ($6 \times 10^{-4} \text{ s}^{-1}$) is almost 3 orders of magnitude slower than that found by Böhmer and co-workers using dynamic NMR techniques (0.26 s^{-1}) for a structurally similar calixarene dimer.^{2c} We attribute the dramatic difference in rates to the additive contribution of three factors: steric congestion at the calixarene lower rim, hydrogen bonding at the lower rim, and the difference in concentration between the studies.

First, the solubilizing groups on the calixarene lower rim that are used in the present work ($-\text{C}_{10}$ alkyl chains) are more bulky than the methyl and $-\text{C}_5$ chains used in the previous dynamic NMR study. These chains may inhibit the calixarene monomer from forming a “pinched cone”¹⁸ as it dissociates, due to steric congestion on the lower rim. This conjecture is supported by the recent observation of very slow dissociation dynamics in tetraurea calixarene dimers that are structurally prevented from forming the pinched cone.¹⁹ Our own conventional NMR kinetic measurements of heterodimer formation and benzene exchange

give a value of $\sim 0.03 \text{ s}^{-1}$ for k_{diss} of **2U·2U** ($-\text{C}_{10}$ chains only on the lower rim) at 4 mM—an order of magnitude slower than previously reported. Second, the amide linker in **2A** and **2D** imparts additional stability by hydrogen bonding to adjacent lower-rim oxygens. This is confirmed by the rate of guest benzene exchange in the dimer **8·8**: by NMR we measured a rate constant of 0.003 s^{-1} , which is another order of magnitude slower than that for the analogous dimer **2U·2U**, and closer to the value measured by FRET. Finally, the concentration of **2** plays a role. The dissociation rate, measured by FRET kinetics, of **2A·2D** varies with the concentration of added **2U**, increasing almost an order of magnitude from 100 nM ($6 \times 10^{-4} \text{ s}^{-1}$) to 1 mM ($3 \times 10^{-3} \text{ s}^{-1}$), where the rate is equivalent to the NMR results on **8·8**. At millimolar concentrations, free **2** is apparently present in sufficient concentration to accelerate the dissociation of the dimer.²⁰ The combination of these three factors explains the disparity between the dynamic NMR measurements and those in the present study.

The association and dissociation rates in benzene reveal unique behavior for the sulfonyl urea **1**. Although its homodimer is the least stable of the three capsules investigated, it dissociates more slowly than aryl urea homodimer **2·2**. Moreover, it is very slow to assemble; its k_{ass} is more than 2 orders of magnitude lower than that of the aryl urea and 6 orders of magnitude lower than the diffusion rate ($\sim 10^9 \text{ M}^{-1} \text{ s}^{-1}$). These data point to a stable sulfonyl urea monomer. Reinhoudt and co-workers were the first to show that calixarene 1,3-bisureas could stabilize the pinched cone conformation through formation of strong intramolecular hydrogen bonds.¹⁸ Modeling of the sulfonyl tetraurea monomer reveals that intramolecular hydrogen bonding is likely between neighboring ureas through participation of the sulfonyl urea oxygens.

Small-Molecule Sensing. The assembly process shown in Figure 1 only occurs in the presence of a suitable guest molecule, and the solvent itself fills that role in the work described above. When the solvent is not a viable guest, then the FRET system may be a sensitive method for small-molecule detection in which the analytes remain chemically unmodified.²¹ We have designed such a system using heterodimers of calixarenes functionalized with aryl ureas **2D** and amino acid-derived ureas **3A**.⁴ These components form a strongly associating dimer in chloroform ($K_{\text{A}} \approx 2 \times 10^7 \text{ M}^{-1}$), but in *p*-xylene both NMR and FRET studies indicate no assembly. The presence of a good guest should trigger capsule formation and a concomitant FRET signal. The results, shown in Figure 7, are promising; in *p*-xylene energy transfer is observed only in the presence of added guest, in this case 3-methylcyclopentanone. When **2D** and **3A** are present in 150 nM concentrations, the threshold concentration for energy transfer is ca. 0.1 mM 3-methylcyclopentanone and assembly is 50% complete at ca. 4 mM added guest. The association constant for the ternary complex is $\sim 3 \times 10^9 \text{ M}^{-2}$, which is considerably higher than that of the assembly in benzene ($\sim 10^6 \text{ M}^{-2}$)—consistent with our observation that 3-methylcyclopentanone is a good guest for the capsule interior. The sensitivity and specificity of the fluorescence signal is advantageous for more complex sensing schemes based on

(20) Even low concentrations of hydrogen-bonding groups have a dramatic effect on the rates of the assembly processes, e.g., dissociation of **1D·2A** in the presence of only 0.3% DMSO occurs in seconds vs hours.

(21) For a review of fluorescence-based sensing, see: Prasanna de Silva, A.; Nimal Gunaratne, H. Q.; Gunlaugsson, T.; Huxley, A. J. M.; McCoy, C. P.; Rademacher, J. T.; Rice, T. E. *Chem. Rev.* **1997**, *97*, 1515–1566. See also (a) Song, X.; Nolan, J.; Swanson, B. I. *J. Am. Chem. Soc.* **1998**, *120*, 11514–11515. (b) Chen, C.-T.; Wagner, H.; Still, W. C. *Science* **1998**, *279*, 851–853. (c) Rothman, J. H.; Still, W. C. *Bioorg. Med. Chem. Lett.* **1999**, *9*, 509–512.

(17) Lomakin, A.; Benedek, G. B.; Castellano, R. K.; Nuckolls, C.; Rebek, J., Jr., unpublished work.

(18) Scheerder, J.; Vreekamp, R. H.; Engbersen, J. F. J.; Verboom, W.; van Duynhoven, J. P. M.; Reinhoudt, D. N. *J. Org. Chem.* **1996**, *61*, 3476–3481.

(19) Brody, M. S.; Rebek, J., Jr., unpublished work.

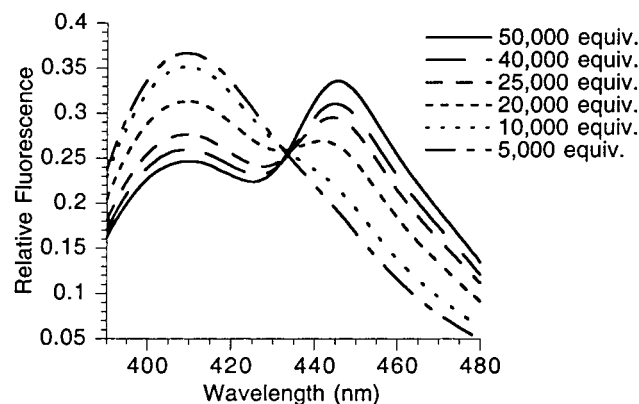


Figure 7. Addition of 3-methylcyclopentanone (equiv) to an equimolar mixture of **2D** and **3A** in *p*-xylene (150 nM). A growing FRET signal indicates assembly nucleation as more guest is added.

combinations of capsules and dyes. Current research efforts are directed along these lines.

Conclusions

FRET techniques, although widely used in biology, have been largely underutilized in molecular recognition studies using synthetic receptors.^{19b,c} They are particularly useful when association constants are high and compound availability is low. The energy transfer methodology is chemically benign—the dyes do not participate in binding, nor are they modified by the assembly process; they act as noninvasive “reporters” of the recognition event. The sensitivity of the technique has revealed behavior and thermodynamic information not accessible at higher concentrations, and its specificity promises greater use in small-molecule sensing.

Experimental Section

Fluorescence Measurements. Measurements were performed on an SLM-AMINCO 8100 spectrofluorometer equipped with a 450 W xenon lamp, an MC200 single-grating excitation monochromator (BP 4 nm), and two single-grating MC200 emission monochromators (T-optics geometry, BP 8 nm). Left and right polarizers were set to the magic angle, 54.7°. Fluorescence is presented in arbitrary units calculated as the ratio of observed emission intensity divided by an internal reference. All measurements were performed at 25.0 ± 0.1 °C. The dyes used showed no susceptibility to photobleaching. Spectrophotometric grade chloroform (stabilized with amylenes) and benzene were purchased from Aldrich and used as received.

Representative Kinetics Measurement. Benzene solutions of 100 nM **1D** and 250 nM **2A** were equilibrated at 25 °C for 15 min. From each solution 1.5 mL was added to a 1 cm quartz cuvette (Hellma). An emission spectrum of the initial reactant mixture was taken. The fluorescence values at the donor (415 nm) and acceptor (455 nm) emission maxima were simultaneously recorded every 90 s using the two emission monochromators. Fluorescence signals were integrated for 10 s, and the excitation signal was closed between acquisitions. An emission spectrum was recorded following the experiment.

General. ¹H NMR (600 MHz) and ¹³C NMR (151 MHz) spectra were recorded on a Bruker DRX-600 spectrometer. Infrared spectra were recorded on a Perkin-Elmer Paragon 1000PC FT-IR spectrometer. Matrix-assisted laser desorption/ionization (MALDI) FTMS experiments were performed on an IonSpec FTMS mass spectrometer. The fast atom bombardment (FAB) positive ion mass spectra were obtained on a VG ZAB-VSE double-focusing high-resolution mass spectrometer. Dichloromethane (CH₂Cl₂) was passed through columns of activated aluminum oxide as described by Grubbs and co-workers prior to use.²² Coumarin 2 and coumarin 343 were purchased from Acros and used without

further purification. All other reagents were purchased from either Aldrich or Fluka and used as received. HCl (g) was bubbled through H₂SO₄ prior to use. The preparations of tetraureas **1U**,^{3a} **2U**,⁵ and **5**⁵ have been described in the literature.

General PyBOP Coupling Procedure. The calixarene monoacid (1 equiv) is dissolved in dimethylformamide (DMF) and treated with PyBOP (1.2 equiv) and NEt₃ (2–10 equivs.). To this is then added the amine (1–1.2 equiv). The coupling reaction is monitored by thin-layer chromatography (TLC) and is generally complete within 1 h. The solvent is removed in vacuo and the residue is dissolved in CH₂Cl₂. After the organic phase is washed with 1 M HCl, 1 M NaOH (except for **1D**), and brine, it is dried over MgSO₄, filtered, and evaporated to give the crude product.

Preparation of Modified Coumarin 2 (6). To coumarin 2 (0.40 g, 1.8 mmol) was added CH₃CN (20 mL), *tert*-butyl *N*-[4-(bromomethyl)benzyl]carbamate²³ (0.37 g, 1.2 mmol), and K₂CO₃ (0.43 g, 3.1 mmol). The mixture was heated to reflux for 36 h. After this time, the mixture was filtered and the filtrate was concentrated to dryness. Addition of MeOH resulted in the precipitation of remaining coumarin 2. This solid was filtered off and the filtrate was concentrated and purified by SiO₂ chromatography (gradient elution, CH₂Cl₂ to 30:1 CH₂Cl₂/MeOH). The desired product was slightly less polar than the starting amine: yield 0.29 g (55%). ¹H NMR (DMF-*d*₇) δ 7.60 (s, 1H), 7.35 (d, 2H, *J* = 8.0 Hz), 7.24 (d, 2H, *J* = 8.0 Hz), 7.24 (m, 1H), 7.02 (s, 1H), 6.19 (s, 1H), 4.33 (s, 2H), 4.22 (d, 2H, *J* = 6.2 Hz), 3.14 (q, 2H, *J* = 6.9 Hz), 2.44 (s, 3H), 2.43 (s, 3H), 1.40 (s, 9H), 1.10 (t, 3H, *J* = 6.9 Hz). ¹³C NMR (DMF-*d*₇) δ 160.80, 156.51, 154.07, 153.56, 152.88, 139.56, 137.65, 129.71, 128.42, 127.45, 127.36, 114.79, 112.25, 108.98, 78.12, 55.32, 47.31, 43.78, 28.17, 18.30, 17.97, 11.80. IR (thin film) 3349, 2975, 1712, 1613, 1512, 1390, 1267, 1248, 1170 cm⁻¹. High-resolution mass spectrometry (HRMS) (FAB; M⁺) calcd for C₂₆H₃₂N₂O₄: 436.2362. Found 436.2368.

The protected amine (0.022 g, 0.050 mmol) was then dissolved in dioxane (10 mL) and treated with HCl (g). After 30 min, the solution was sparged with N₂ and concentrated to dryness. The hygroscopic, off-white powder obtained was used without further purification (quant.). HRMS (FAB; M + H⁺) calcd for C₂₁H₂₅N₂O₂: 337.1916. Found 337.1920.

Sulfonyl Urea Donor (1D). The calixarene monoacid **4**²⁴ (0.10 g, 0.13 mmol) was combined with the coumarin amine hydrochloride **6** (0.028 g, 0.16 mmol), PyBOP (0.036 g, 0.16 mmol), and NEt₃ (80 μL, 1.3 mmol) in DMF (10 mL). The initial oily product obtained was triturated with MeOH to furnish a white powder (0.081 g, 69%). ¹H NMR (DMF-*d*₇) δ 10.40 (s, 1H), 10.35 (s, 1H), 10.30 (s, 2H), 8.65 (s, 1H), 8.60 (s, 1H), 8.53 (s, 2H), 8.45 (t, 1H, *J* = 6.0 Hz), 7.98–7.94 (m, 8H), 7.58 (s, 1H), 7.49–7.46 (m, 8H), 7.35 (d, 2H, *J* = 8.0 Hz), 7.24 (d, 2H, *J* = 8.0 Hz), 6.99 (s, 1H), 6.76 (s, 2H), 6.75 (s, 2H), 6.62 (s, 4H), 6.13 (s, 1H), 4.54 (m, 4H), 4.39 (d, 2H, *J* = 13.4 Hz), 4.32 (s, 2H), 4.30 (d, 2H, *J* = 13.1 Hz), 3.83–3.72 (m, 6H), 3.12 (q, 2H, *J* = 6.8 Hz), 3.05 (d, 2H, *J* = 13.1 Hz), 3.04 (d, 2H, *J* = 13.6 Hz), 2.47–2.45 (m, 12H), 2.42 (s, 3H), 2.39 (s, 3H), 1.81 (m, 2H), 1.73 (m, 4H), 1.36–1.26 (m, 42H), 1.09 (t, 3H, *J* = 7.0 Hz), 0.88–0.85 (m, 9H). ¹³C NMR (DMF-*d*₇) δ 169.27, 160.74, 154.49, 153.97, 153.46, 152.87, 152.61, 152.31, 149.98, 144.38, 138.31, 138.21, 135.47, 135.19, 134.63, 134.55, 133.31, 132.85, 129.79, 129.76, 128.58, 128.16, 127.43, 127.18, 120.02, 119.92, 119.76, 114.87, 112.33, 109.09, 75.73, 75.18, 74.64, 55.40, 47.33, 42.21, 32.16, 31.77, 31.51, 31.25, 26.48, 26.30, 22.84, 21.01, 13.98, 11.77. IR (thin film) 3340, 2924, 2853, 1715, 1694, 1613, 1552, 1464, 1346, 1216, 1164, 1091, 1056, 895 cm⁻¹. Low-resolution mass spectra (LRMS) electron spray ionization (ESI); M + H⁺ calcd for C₁₁₃H₁₄₁N₁₀O₁₉S₄: 2071. Found 2071.

Aryl Urea Donor (2D). The calixarene monoacid **5**⁵ (0.054 g, 0.036 mmol) was combined with the coumarin amine hydrochloride **6** (0.015 g, 0.036 mmol), PyBOP (0.023 g, 0.043 mmol), and NEt₃ (30 μL, 0.22 mmol) in DMF (5 mL). The crude product was purified by chromatography on SiO₂ (15:1 CH₂Cl₂/MeOH) to give a white powder (0.032 g, 49%). ¹H NMR (DMF-*d*₇) δ 8.63 (t, 1H, *J* = 6.1 Hz), 8.51 (s, 1H), 8.50 (s, 1H), 8.48 (s, 1H), 8.44 (s, 1H), 8.35 (s, 2H), 8.32 (s, 2H), 7.60

(22) Pangborn, A. B.; Giardello, M. A.; Grubbs, R. H.; Rosen, R. K.; Timmers, F. J. *Organometallics* **1996**, *15*, 1518–1520.

(23) Niu, J.; Lawrence, D. S. *J. Biol. Chem.* **1997**, *272*, 1493–1499.

(24) See the Supporting Information for synthetic details.

(s, 1H), 7.43–7.38 (m, 6H), 7.32–7.29 (m, 6H), 7.11 (d, 2H, $J = 8.5$ Hz), 7.10 (d, 2H, $J = 8.5$ Hz), 7.08–7.06 (m, 8H), 7.02 (s, 1H), 6.76 (s, 2H), 6.75 (s, 2H), 6.18 (s, 1H), 4.71 (s, 2H), 4.65 (d, 2H, $J = 6.0$ Hz), 4.49 (d, 2H, $J = 13.4$ Hz), 4.43 (d, 2H, $J = 13.1$ Hz), 4.34 (s, 2H), 3.91 (t, 2H, $J = 7.5$ Hz), 3.86–3.78 (m, 4H), 3.21–3.16 (m, 4H), 3.14 (q, 2H, $J = 7.0$ Hz), 2.45 (s, 3H), 2.42 (s, 3H), 2.26 (s, 6H), 2.25 (s, 6H), 1.91 (m, 2H), 1.79 (m, 4H), 1.41–1.30 (m, 42H), 1.10 (t, 3H, $J = 6.5$ Hz), 0.90–0.87 (m, 9H). ^{13}C NMR (DMF- d_7) δ 169.84, 160.77, 154.00, 153.47, 153.29, 153.26, 153.22, 152.90, 152.40, 151.86, 151.20, 138.44, 138.33, 138.29, 138.25, 137.86, 135.82, 134.93, 134.87, 134.67, 134.61, 134.21, 130.99, 130.94, 130.76, 129.77, 129.46, 129.37, 128.68, 127.43, 127.12, 119.36, 119.16, 118.98, 118.91, 118.49, 118.47, 118.29, 114.90, 112.37, 109.15, 75.83, 75.12, 74.78, 55.51, 47.28, 42.25, 32.19, 31.86, 31.57, 30.41, 30.22, 30.14, 30.09, 29.99, 29.67, 26.54, 26.41, 22.87, 20.23, 20.21, 18.33, 17.99, 14.01, 11.78. IR (thin film) 3341, 2924, 2854, 1715, 1667, 1634, 1607, 1555, 1515, 1476, 1417, 1315, 1212 cm^{-1} . HRMS (MALDI–FTMS; $\text{M} + \text{Na}^+$) calcd for $\text{C}_{113}\text{H}_{140}\text{N}_{10}\text{O}_{11}\text{Na}$: 1836.0601. Found: 1836.0584.

tert-Butoxycarbonyl (BOC)–Protected Tetraaryl Urea (7). The calixarene acid **5** (0.30 g, 0.20 mmol) was combined with mono-BOC ethylenediamine (38 μL , 0.24 mmol), PyBOP (0.13 g, 0.24 mmol), and NEt_3 (56 mL, 0.40 mmol) in DMF (10 mL). The crude product, following trituration with MeOH, was further purified by precipitation from THF with MeOH to give a white powder (0.20 g, 61%). ^1H NMR (DMF- d_7) δ 8.49 (s, 2H), 8.48 (s, 1H), 8.44 (s, 1H), 8.39 (t, 1H, $J = 5.7$ Hz), 8.31 (d, 4H, $J = 8.3$ Hz), 7.39 (d, 4H, $J = 8.2$ Hz), 7.29 (d, 4H, $J = 8.3$ Hz), 7.11–7.06 (m, 12H), 6.98 (t, 1H, $J = 5.8$ Hz), 6.76 (m, 2H), 6.75 (m, 2H), 4.62 (s, 2H), 4.51 (d, 2H, $J = 13.5$ Hz), 4.45 (d, 2H, $J = 13.1$ Hz), 4.03 (m, 2H), 3.95 (m, 2H), 3.90 (m, 2H), 3.51 (m, 2H), 3.30 (m, 2H), 3.25 (d, 2H, $J = 13.7$ Hz), 3.18 (d, 2H, $J = 13.3$ Hz), 2.26 (s, 6H), 2.25 (s, 6H), 1.89 (m, 6H), 1.47–1.29 (m, 42H), 1.43 (s, 9H), 0.91–0.88 (m, 9H). ^{13}C NMR (DMF- d_7) δ 170.04, 156.47, 153.28, 153.24, 153.21, 152.65, 151.82, 151.15, 138.32, 138.28, 138.22, 135.91, 134.87, 134.84, 134.68, 134.60, 134.15, 130.98, 130.93, 130.74, 129.45, 129.35, 119.33, 119.13, 118.99, 118.95, 118.48, 118.27, 78.08, 75.95, 75.04, 74.82, 40.50, 39.51, 32.17, 32.15, 31.86, 31.63, 30.34, 30.18, 30.12, 30.11, 29.99, 29.94, 28.22, 26.50, 26.46, 22.85, 20.22, 20.20, 14.00. IR (thin film) 3351, 2924, 2854, 1715, 1667, 1607, 1552, 1514, 1476, 1316, 1212 cm^{-1} . HRMS (MALDI–FTMS; $\text{M} + \text{Na}^+$) calcd for $\text{C}_{99}\text{H}_{132}\text{N}_{10}\text{O}_{11}\text{Na}$: 1659.9975. Found: 1659.9948.

Deprotection (8). The protected amine **7** (0.10 g, 0.061 mmol) was dissolved in dioxane (15 mL) and treated with HCl (g). After 30 min, the solution was sparged with N_2 and concentrated to dryness. The oily solid obtained was used without further purification (quant.). HRMS (FAB; $\text{M} + \text{Cs}^+$) calcd for $\text{C}_{94}\text{H}_{124}\text{N}_{10}\text{O}_9\text{Cs}$: 1669.8607. Found: 1669.8709.

Acceptor Aryl Urea (2A). The calixarene amine hydrochloride **8** (0.060 g, 0.039 mmol) was combined with coumarin 343 (0.011 g, 0.039 mmol), PyBOP (0.024 g, 0.047 mmol), and NEt_3 (11 μL , 0.078 mmol) in DMF (5 mL). The crude product was purified by chromatography on SiO_2 (10:1 $\text{CH}_2\text{Cl}_2/\text{MeOH}$) to give a bright yellow powder (0.046 g, 65%). ^1H NMR (600 MHz, DMF- d_7) δ 9.04 (t, 1H, $J = 5.8$ Hz), 8.59 (s, 1H), 8.58 (m, 2H), 8.52 (s, 1H), 8.50 (s, 2H), 8.49 (s, 1H), 8.40 (t, 1H, $J = 5.4$ Hz), 8.38 (s, 2H), 7.39 (d, 2H, $J = 8.1$ Hz), 7.38 (d, 2H, $J = 8.2$ Hz), 7.31 (d, 4H, $J = 8.3$ Hz), 7.25 (s, 1H), 7.09 (d, 2H, $J = 7.9$ Hz), 7.08 (d, 2H, $J = 8.0$ Hz), 7.05 (d, 4H, $J = 8.3$ Hz), 7.02 (m, 4H), 6.76 (m, 4H), 4.61 (s, 2H), 4.51 (d, 2H, $J = 13.5$ Hz), 4.44 (d, 2H, $J = 13.1$ Hz), 4.02 (m, 2H), 3.95 (m, 2H), 3.88 (m, 2H), 3.70 (m, 2H), 3.63 (m, 2H), 3.37 (m, 4H), 3.22 (d, 2H, $J = 13.7$ Hz), 3.16 (d, 2H, $J = 13.3$ Hz), 2.80 (m, 4H), 2.26 (s, 3H), 2.25 (s, 3H), 2.24 (s, 6H), 1.97–1.86 (m, 10H), 1.42–1.27 (m, 42H), 0.88–0.86 (m, 9H). ^{13}C NMR (DMF- d_7) δ 170.01, 163.65, 153.23, 152.97, 152.39, 151.80, 151.26, 148.66, 147.98, 138.32, 138.26, 135.73, 135.05, 134.86, 134.67, 134.59, 134.51, 134.41, 130.91, 130.87, 130.74, 129.42, 129.36, 127.60, 120.19, 119.37, 119.20, 119.06, 118.42, 118.29, 108.76, 108.14, 105.39, 75.88, 75.16, 74.78, 50.15, 49.63, 39.76, 39.31, 32.18, 31.86, 31.61, 30.41, 27.42, 26.55, 26.46, 22.86, 21.19, 20.22, 14.00. IR (thin film) 3339, 2924, 2853, 1666, 1606, 1552, 1515, 1476, 1311, 1210 cm^{-1} . HRMS (FAB; $\text{M} + \text{Cs}^+$) calcd for $\text{C}_{110}\text{H}_{137}\text{N}_{11}\text{O}_{12}\text{Cs}$: 1936.9503. Found: 1936.9618.

Acknowledgment. We are grateful to the Skaggs Research Foundation, the National Institutes of Health (NIH), and the National Aeronautics and Space Administration (NASA) for financial support. R.K.C. thanks the American Chemical Society, Division of Organic Chemistry, and Schering-Plough for a graduate research fellowship (1998–1999). S.L.C. and C.N. thank the NIH for postdoctoral fellowships. We are indebted to Professor David P. Millar (TSRI) and his staff for the use of their equipment and for insightful discussions. We also thank Professor Jamie R. Williamson (TSRI) for helpful advice.

Supporting Information Available: Supporting Information Available: Full synthetic details including the characterization of all precursors and final compounds including **3A**, **4**, **9D**, and **9A**. Also DMSO titration experiments performed with the control samples (PDF). This material is available free of charge via the Internet at <http://pubs.acs.org>.

JA994397M